McKibben Artificial Muscles: Pneumatic Actuators with Biomechanical Intelligence

Glenn K. Klute
Dept. of Bioengineering

Joseph M. Czerniecki
Dept. of Rehabilitation Medicine

Blake Hannaford
Dept. of Electrical Engineering

University of Washington
Seattle, WA 98195-2500
206/616-4936 voice
206/543-3842 fax
gklute@u.washington.edu
http://rcs.ee.washington.edu/BRL/

ABSTRACT

This paper reports on the design of a biorobotic actuator. Biological requirements are developed from published reports in the muscle physiology literature whose parameters are extracted and applied in the form of the Hill muscle model. Data from several vertebrate species (rat, frog, cat, and human) are used to evaluate the performance of a McKibben pneumatic actuator. The experimental results show the force-length properties of the actuator are muscle-like, but the force-velocity properties are not. The design of a hydraulic damper with fixed orifices, placed in parallel with the McKibben actuator, is proposed to improve the force-velocity performance. Simulation results of this practical design indicate a significant improvement.

1 INTRODUCTION

The growth era of robotics, through the mid-1980's, was heralded by the introduction of automation into labor intensive industries. As with any market inefficiency, the easy problems were tackled first to maximize the return on investment. However, as the robotic industry's growth declined in the 1990's, it was clear the hard problems were left. One of the most challenging problems is the ability of a robot to productively interact in an uncontrolled environment. Human labor remains the most effective means of solving this problem.

The "Biorobotic" approach to solving this problem is to emulate the very properties that allow humans to be successful. Each component of the biorobotic system must incorporate as many of the known aspects of such diverse areas as neuromuscular physiology, biomechanics, and cognition to name a few, into the design of sensors, actuators, circuits, processors, and control algorithms (see figure 1).

The research presented in this paper describes the development of one component of the biorobotic system: the actuator. Our approach uses a pneumatic device that was developed in the 1950's as an orthotic appliance for polio patients' by J. L. McKibben [2]. Powered by compressed gas, the actuator is made from an inflatable inner bladder sheathed with a double helical weave which contracts lengthwise when expanded radially (see figure 2). This paper begins by identifying the performance of biological muscle to provide design requirements and desired performance specifications for artificial muscle actuators. Experimental results from tests with the McKibben actuator will then be presented for comparison purposes. Faced with an obvious discrepancy, we will propose a practical solution. The simulation results of our proposed solution appear reasonable.

2 BIOLOGICAL MUSCLE

Biological muscle can be modeled as an actuator whose output force is a function of length, velocity, and level of activation. The muscle physiology literature contains numerous reports identifying the relationship between force and length during isometric contractions (constant length) when the activation is maximal. Figure 3 presents this relationship in a dimensionless form for rat, frog, cat, and human muscles, as well as for the McKibben actuator [3-6]. Along the ordinate, the instantaneous output force at any length is normalized by the output force at the muscle's *in-vivo* resting length, while along the abscissa, the instantaneous length is normalized by the *in-vivo* resting length. As is readily observable, the passive properties of muscle allow it to stretch far beyond its *in-vivo* resting length, while the McKibben actuator cannot. However, for lengths less than resting, the McKibben actuator provides a first order approximation of biological muscle.

Another important property of biological muscle that cannot be ignored is the relationship between force and velocity. In general, it is well known that at a constant level of activation, the output force of biological muscle drops significantly as contraction velocities increase. Numerous models of this phenomenon have been proposed, but the most enduring has been that of Hill [9].

The Hill muscle model captures perhaps 90 percent of what is relevant for organism level biomechanics with a simple, hyperbolic equation. The generic form of this is equation is given by:

$$[F_m + a][V_m + b] = [F_{m,o} + a]b \qquad (1)$$

where F_m is the instantaneous muscle force, V_m is the instantaneous muscle velocity, and $F_{m,o}$ is the isometric muscle force at the muscle's "resting" length ($l_{m,o}$). The constants a and b are empirically determined and depend not only on the species of interest, but also on the type of muscle fiber within a species.

Values from the muscle physiology literature for the parameters in equation (1) are given in table 1 for the rat, frog, cat, and human [7, 8, 10-12]. Muscle physiology data such as this has been used to model gait, musculo-skeletal diseases, and development of motor control theories to name a few. To compare how biomechanic investigators have used this type of information, table 1 also includes values from several of these models [13-16].

Examination of the parameters in table 1 clearly indicates there is a wide range of possible values. Figure 4 plots the results of equation (1) and data from table 1 using points for the animal data and lines for the biomechanic models. The figure shows significant variation across animals as well as variation among published muscle models purporting to portray the performance of humans.

In order to identify the range of performance that would be acceptable for a biorobotic actuator, a reasonable envelope based on table 1 data is given by:

$$0.12 \le a/F_{m,o} \le 0.41 \qquad (2a)$$

$$0.22 \le b/V_{m,o} \le 0.52 \qquad (2b)$$

for $F_m/F_{m,o} \le 1.0$ and $V_m/V_{m,o} \le 1.0$.

3 McKIBBEN ACTUATOR

The McKibben actuator has been suggested as an actuator whose performance is similar to biological muscle [17]. As shown in figure 3, this is true for the force-length relationship, but little is known regarding the force-velocity relationship. To provide data for comparing with biological muscle, we conducted an experiment to measure the force-velocity properties of the McKibben actuator.

3.1 EXPERIMENTAL METHODS

To measure the force-velocity properties of the McKibben actuator, we conducted a series of experiments with an axial-torsional Bionix™ (MTS Systems Corp.,

Minnesota, USA) tensile testing instrument. Each experiment measured the force output at a constant pressure over the working contraction range at various velocities. We limited the input pressure to a maximum of 5 bar out of consideration for typical industrial air compressors. To ensure maintenance of a constant pressure while the actuator changed shape during a contraction, we attached a pressure vessel whose volume was significantly larger than the actuator (4000:1 minimum volume ratio). The instrument's digital controller was used to input velocity ranges from 0 mm/s to 300 mm/s. Up to 500 mm/s is possible, however, instantaneous fluctuations in velocity of 15 percent were measured during trails at 500 mm/s. The magnitude of these fluctuations decreased at lower velocities, and was less than 9 percent at 300 mm/s and 6 percent at 200 mm/sec. This anomaly is thought to arise from the hydraulic pump.

The actuator whose results are presented here was constructed with a natural latex rubber bladder with interior diameter of 12.8 mm (3/8 in) and a 1.6 mm (1/16 in) wall thickness. The braid had a "nominal diameter" of 31.75 mm (1.25 in) based on Alpha Wire Corporation's product specifications (New Jersey, U.S.A.). Although not shown, we also constructed both smaller and larger actuators whose performance was similar. To minimize tip-effects at the actuator's ends, the actuators were constructed such that their length to diameter ratios were at least 14.

3.2 EXPERIMENTAL RESULTS

The experimentally measured output force of the McKibben actuator, plotted as a function of both length and velocity, is shown in figure 5. To compare with the "enveloped" properties of biological muscle (equations 1 and 2), a portion of this data is re-plotted as force versus velocity at a constant length in figure 6. In the muscle physiology literature, it is common to select the muscle's *in-vivo* resting length as this constant value; however, our test set-up requires a few milliseconds to reach the target velocity. Therefore, in figure 6, the experimental data and biological model values (F_m and V_m) were taken when the actuator's length (l_m) was slightly shorter than the resting length (such that $l_m = 0.96 l_{m,o}$). The maximum force of the McKibben actuator ($F_{m,o}$) was 734 N under static conditions (0 mm/s), and decreased with increasing velocity. At 300 mm/s, the output force was 690 N, a decrease of only 6 percent.

3.3 EXPERIMENTAL DISCUSSION

From the experimental results, it is evident that the McKibben actuator has only a small amount of natural damping. The output force is clearly a function of length, but changes in velocity have only a small effect. When compared to a well-known model of biological muscle, it is clear that the current McKibben actuator has significantly different performance than biological muscle with respect to velocity. By adding additional damping, it may be possible to create an improved actuator whose properties are muscle-like with respect to both length and velocity.

4 PARALLEL DAMPING ELEMENT

One method for increasing the damping is to add a hydraulic damper in parallel to the pneumatic McKibben actuator as shown in figure 7. An actively controlled orifice with a fast response might be able to perfectly mimic biological muscle. However, such an orifice would add a significant level of complexity to the system. Our approach is to add a passive, fixed orifice damper in order to minimize the additional complexity. Adopting this approach results in a simpler system, albeit with a corresponding loss in potential performance.

For a damper in parallel with the McKibben actuator, the desired damping force (F_{hyd}) is simply:

$$F_{hyd} = F_{McK} - F_m \tag{3}$$

where F_{McK} is the McKibben actuator output force whose value can either be taken from experiment or from a model published elsewhere [3]. F_m is the force produced by biological muscle, modeled by equations (1) and (2).

For small hydraulic components, a common design constraint is the maximum allowable cylinder pressure (P_{cyl}) identified by the manufacturer. This constraint, along with the desired damping force, allows calculation of the hydraulic cylinder's inside diameter (ϕ_1):

$$F_{hyd} = \left(\frac{\pi \phi_1^2}{4} \right) P_{cyl} \tag{4}.$$

For a cylinder with a maximum allowable pressure of 6.8 MPa (1000 psi) and a maximum damping force of approximately ~700 N, the minimum cylinder diameter is 11.4 mm. A number of small bore cylinders are commercially available.

Approaching the problem of calculating the desired orifice size using conservation of energy, Bernoulli's equation can be written as:

$$\frac{P_1}{\rho} + \frac{v_1^2}{2g} = \frac{P_2}{\rho} + \frac{v_2^2}{2g} \tag{5}$$

where P is pressure, v is fluid velocity, ρ is the fluid density, and g is gravity. The subscripts 1 and 2 refer to cylinder and orifice locations.

Furthermore, conservation of mass ($\dot{m}$) demands:

$$\dot{m}_1 = \dot{m}_2 \tag{6}$$

such that:

$$\rho A_1 v_1 = \rho A_2 v_2 \tag{7}$$

where A is the cross-sectional area. An empirical enhancement to this equation is the multiplication of a discharge coefficient (C_d) to the right side of equation (7). This coefficient accounts for *vena contracture* at the orifice, an effective reduction in cross-sectional area. The value of this coefficient can be as low as 0.61 for very high Reynolds numbers, however, we have set this parameter to 1.0 for our simulations but plan future experimental measurements.

Substitution and simplification yields an equation for determining the ideal orifice size:

$$\phi_2^4 = \frac{\pi v_1^2 \phi_1^6 \rho}{8 F_d C_d^2 + \rho \pi \phi_1^2 v_1^2 C_d^2} \tag{8}$$

where ϕ_2 is the orifice diameter.

Equation (8) gives the instantaneous orifice diameter required to obtain the precise amount of damping desired. However, as previously noted, such an orifice would add a significant level of complexity to the system. The damping force generated by a fixed orifice damper can be calculated from:

$$F_{hyd} = \frac{\pi \rho \phi_1^2 v_1^2}{8} \left(\frac{\phi_1^4}{C_d^2 \phi_2^4} - 1 \right) \tag{9}$$

Since the hydraulic damping force is a function of the square of the velocity, the shape of the force v. velocity curve will be convex instead of the desired concavity exhibited by biological muscle. However, if the fixed orifice size is selected based on the expected range of the application's velocity, the effect of this error can be minimized.

5 SIMULATION RESULTS

Combining the experimental data (F_{McK}) and the damper force (F_{hyd}) as predicted by equation (9), the ability to generate muscle-like output can now be assessed.

If a perfect, Hill-like damper were placed in parallel with the McKibben actuator, the results would be as

shown in figure 8. This perfect damper relies on an orifice whose diameter can be varied instantaneously. A design based on a fixed orifice would actually require two separate orifices due to differences in volume between the rod and bore sides of the cylinder. Simulation results, predicting output force as a function of both length and velocity, are shown in figure 9 for the orifice, cylinder, and hydraulic fluid values given in table 2.

6 DISCUSSION

The fixed orifice damper, in parallel with a McKibben actuator, provides a first order approximation to the desired Hill model damping of biological muscle. However, identification of a number of caveats is in order. The hydraulic model presented here (equations 5-9) is simple model intended to capture the significant factors for design purposes. This model ignores losses due to piston rod lipseal friction, frictional losses within the hydraulic lines, the effects of *vena contracture* (ignored when $C_d = 1.0$), and other sources. Furthermore, many of these losses are a function of the Reynolds number. In this system, the Reynolds number varies widely depending on location and actuator contraction velocity. Lastly, the biological model (equations 1 and 2) is valid only for concentric (shortening) muscle contractions and ignores other factors such as parallel and series elasticity.

Refinements to the proposed system can certainly be introduced such as stepper motor controlled needle valves or passive orifices constructed from materials that deform under pressure. The accuracy of the objective function, based on biological muscle, can also be improved by considering differences between contraction direction and effects of activation level.

7 CONCLUSIONS

In spite of differences across species, the Hill muscle model serves as an adequate standard for the design of biorobotic actuators. By enveloping the performance, a range can be specified and used to evaluate an actuator's performance. The McKibben actuator, whose current performance is shown to be sufficient only in terms of its force-length relationship, can be placed in parallel with a hydraulic damper to achieve an appreciable fraction of the desired force-velocity relationship. Simulation results show the actuator-damper system behaves in a muscle-like way and our future work involves construction of this actuator-damper system for use in a lower limb prosthetic device.

REFERENCES

[1] S Franklin, *Artificial Minds*, MIT Press, Cambridge, MA, 1997.

[2] VL Nickel, J Perry, and AL Garrett, "Development of useful function in the severely paralyzed hand," *Journal of Bone and Joint Surgery*, Vol. 45A, No. 5, pp. 933-952, 1963.

[3] GK Klute and B Hannaford, "Modeling pneumatic McKibben artificial muscle actuators: approaches and experimental results," submitted for review, *Journal of Dynamic Systems, Measurements, and Control*, November 1998.

[4] AS Bahler, "Modeling of mammalian skeletal muscle," *IEEE Transactions of Bio-Medical Engineering*, BME-15(4):249-257, 1968.

[5] AS Bahler, "Series elastic component of mammalian skeletal muscle," American Journal of Physiology, 213(6):1560-1564, 1967.

[6] DR Wilkie, "The mechanical properties of muscle," *British Medical Bulletin*, 12(3):177-182, 1956.

[7] HL McCrorey, HH Gale, and NR Alpert, "Mechanical properties of the cat tenuissimus muscle," *American Journal of Physiology*, 210:114-120, 1966.

[8] HJ Ralston, MJ Polissar, VT Inman, JR Close, and B Feinstein, "Dynamic features of human isolated voluntary muscle in isometric and free contractions," *Journal of Applied Physiology*, 1(7):526-533, 1949.

[9] AV Hill, "The heat of shortening and the dynamic constants of muscle," *Proceedings of the Royal Society*, B126:136-195, 1938.

[10] JB Wells, "Comparison of mechanical properties between slow and fast mammalian muscle," *Journal of Physiology*, 18:252-269, 1965.

[11] BC Abbott and DR Wilkie, "The relation between velocity of shortening and the tension-length curve of skeletal muscle," *Journal of Physiology*, 120:214-223, 1953.

[12] DR Wilkie, "The relation between force and velocity in human muscle," *Journal of Physiology*, K110:248-280.

[13] RD Woittiez, PA Huijing, HBK Boom, and RH Rozendal, "A three-dimensional muscle model: a quantified relation between form and function of skeletal muscles," *Journal of Morphology*, 182:95-113, 1984.

[14] MF Bobbert, PA Huijing, and GJ van Ingen Schenau, "A model of the human triceps surae muscle-tendon complex applied to jumping," *Journal of Biomechanics*, 19(11):887-898, 1986.

[15] MF Bobbert and GJ van Ingen Schenau, "Isokinetic plantar flexion: experimental results and model calculations, *Journal of Biomechanics*, 23(2):105-119, 1990.

[16] AL Hof and JW van den Berg, "EMG to force processing. II: estimation of parameters of the Hill muscle model for the human triceps surae by means of a calf-ergometer," *Journal of Biomechanics*, 14:759-770, 1981.

[17] CP Chou and B Hannaford, "Measurement and modeling of artificial muscles," *IEEE Transactions on Robotics and Automation,* Vol. 12, pp. 90-102, 1996.

TABLES and FIGURES

Table 1: Force v. velocity data from the muscle physiology literature for use in equation (1). See text for explanation of parameters.

Animal Model	$a/F_{m,o}$ - none	$F_{m,o}$ - N	$b/V_{m,o}$ - none	$V_{m,o}$ mm/s
Rat[1]	0.356	4.30	0.38	144
Frog[2]	0.27	0.67	0.28	42
Cat[3]	0.27	0.18	0.30	191
Human[4]	0.81	200	0.81	1115
Skeletal Muscle Model[5]	0.224		0.224	
Human[6]	0.41	3000	0.39	756
Human[7]	0.41	2430	0.41	780
Human[8]	0.12		0.12	

[1]Rat *tibialis anterior* muscle at 38 degrees C [10, table 1].

[2]Frog *sartorius* muscle at 0 degrees C [11, figure 5].

[3]Cat *tenuissimus* muscle at 37 degrees C [7, figure 1].

[4]Human *pectoralis major in-vivo*, sternal portion at 37 degrees C [8, figure 1; but see also 12].

[5]Model of generic skeletal muscle [13, equation A-22 and B-8]. Woittiez's dimensionless model did not require the specification of $F_{m,o}$ or $V_{m,o}$.

[6]Model of human *triceps surae* [14].

[7]Model of human *triceps surae* [15].

[8]Model of human *triceps surae* [16]. Hof and ven den Berg's model did not require the specification of $F_{m,o}$ or $V_{m,o}$.

Table 2: Hydraulic parameters used in conjunction with Bernoulli's equation to design the damping element.

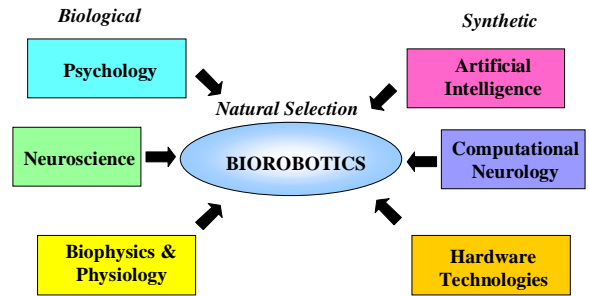| Parameter	Value - units
P_{cyl}	1000 psi max
ρ (mineral oil)	900 kg/m^3
ϕ_1	22.225 mm (7/8 in)
ϕ_2 bore side of cylinder	1.5 mm
ϕ_2 rod side of cylinder	1.3 mm

Figure 1: Biological and synthetic aspects of biorobotic systems [adapted from 1].
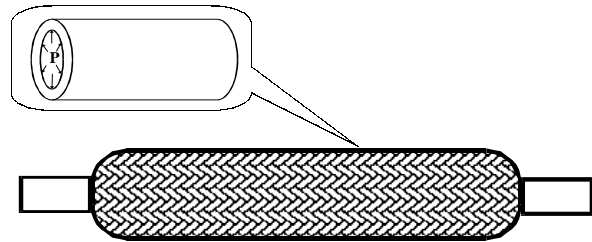

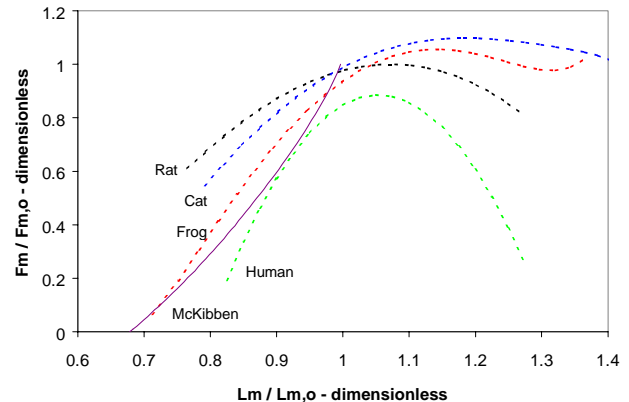Figure 2: McKibben actuator with exterior braid and inner elastic bladder.

Figure 3: The dimensionless relationship between force and length under isometric conditions at maximal activation for various animals as well as a McKibben actuator pressurized to 5 bar.
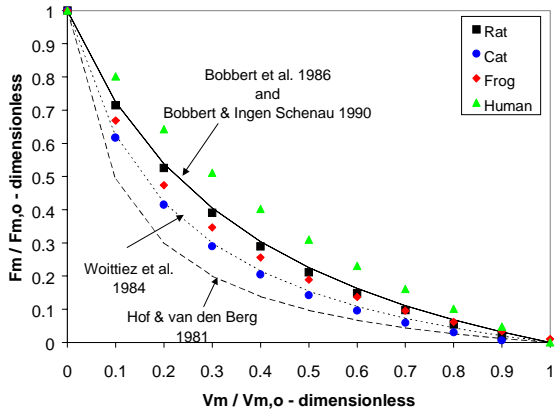
Figure 4: Predicted output force over a muscle's velocity range for four different animals and four published biomechanic models.

Figure 7: A hydraulic damper with orifice flow control valves in parallel with a McKibben actuator.
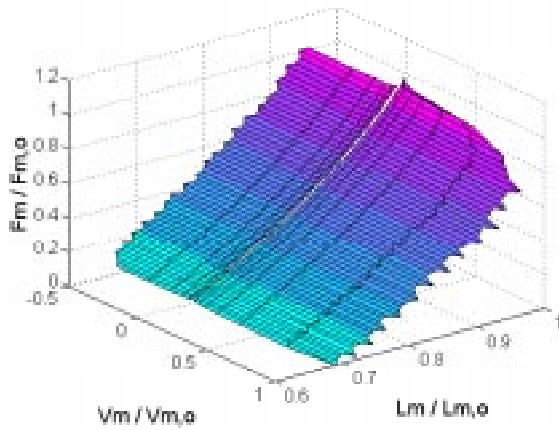

Figure 5: McKibben experimental data plotted as a function of both length and velocity. The ripples along a specific velocity are artifacts of the hydraulic pump used in the testing instrument.
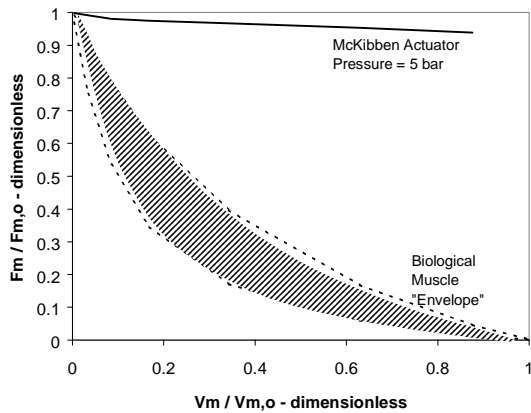

Figure 8: Predicted output force of a McKibben actuator in parallel with perfect, Hill-like damper.

Figure 6: McKibben actuator force output as a function of velocity compared with animal "envelope." The length of the muscle and actuator for which these curves are plotted are explained in the text (section 3.2).
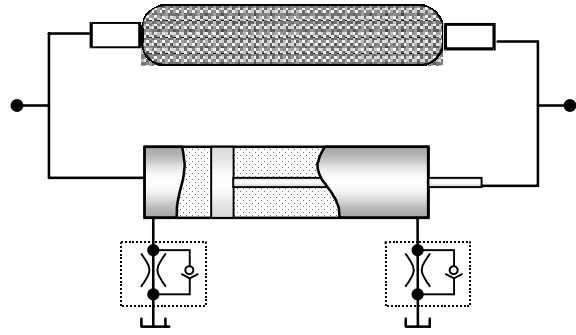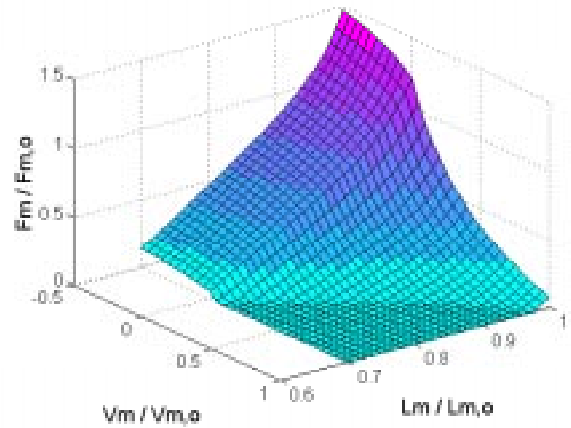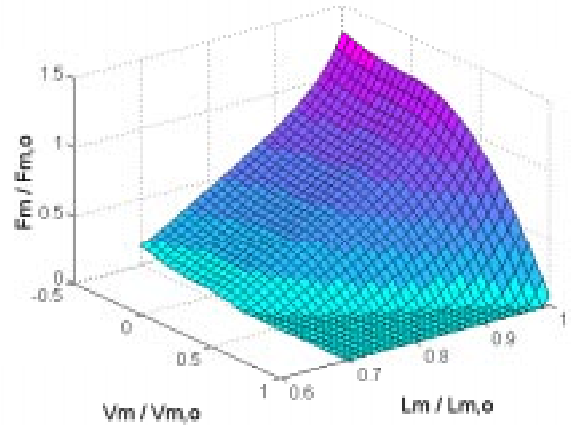

Figure 9: Predicted output force of a McKibben actuator in parallel with a passive, fixed orifice hydraulic damper.